J Math Chem (2015) 53:2123–2136
DOI 10.1007/s10910-015-0542-2

ORIGINAL PAPER

Three mean-field models for bimolecular reactions proceeding on planar supported catalysts

V. Skakauskas[1] · **P. Katauskis**[1]

Received: 26 January 2015 / Accepted: 11 August 2015 / Published online: 19 August 2015

Abstract The kinetics of $A_1 + A_2 \rightarrow A_1A_2$ reaction on supported catalysts is investigated numerically using three phenomenological models. The first of them is based on PDEs and includes: the bulk diffusion of both reactants from a bounded vessel towards the adsorbent and the product bulk one into the same vessel, adsorption and desorption of molecules of both reactants, and surface diffusion of adsorbed particles described by the diffusion flux based on the particle jumping into a nearest vacant adsorption site. The second model based on the ODEs is derived by averaging of the first one. The third mixed model is based on the PDEs for the bulk diffusion of both reactants and ODEs for the adsorbates surface diffusion on the supported catalyst which is composed of the active in reaction catalyst particle and inactive support. All three models are solved numerically and their results are compared. Two distinct arrangements of the adsorption sites are used for numerical calculations: (i) concentrations of the adsorption sites of the catalyst particle and support are equal, (ii) the total amount of adsorption sites of the active and inactive in reaction surface parts are the same. Calculations are performed for the case where: (i) molecules of both reactants adsorb only on the support and (ii) particles of one reactant adsorb on the active part while molecules of the other one adsorb on the support. The influence of the surface diffusivity, jump rate constants of the escaped particles of both adsorbates via the catalyst-support interface, and size of the active catalyst particle (or size-dependent distribution of active sites in the second case of their arrangement) on the catalytic reactivity of the supported catalyst is studied.

✉ V. Skakauskas
vladas.skakauskas@maf.vu.lt

[1] Faculty of Mathematics and Informatics, Vilnius University, Naugarduko 24, 03225 Vilnius, Lithuania

Keywords Heterogeneous reactions · Adsorption · Desorption · Surface diffusion · Spillover

1 Introduction

Modelling of catalytic processes plays a central role in study of kinetics in heterogeneous catalysis and catalysts design in chemical industry [1–5]. Real catalysts consist of small active particles placed on inactive in reaction supports. One of kinetic effects associated with small catalyst particles on a support is the spillover effect. It is caused by the fact that parts of the surface which are inactive in the surface reaction can be active for other processes that occur during the catalytic process, i.e. adsorption-desorption process and increase or decrease concentrations of either substrate or product particles on active parts of the surface through the diffusion of the adsorbed reactant particles across the interface between the catalyst particles and the support [1,6,7].

The bibliography of the current state of theoretical research of reactions with spillover effects include: (i) papers based on the Monte Carlo simulations technique [6,8–10], (ii) numerical solving of mean-field models [11–16], and (iii) the analytical description of such effect [2,17]. In [9], the uni-molecular $A \rightarrow B$ and bimolecular $2A \rightarrow B$ reversible reactions occuring on the composite catalyst surface are studied. In [6,8,10], the three-molecular $2A + B_2 \rightarrow 2AB$ reaction is considered. In [11,12], these reactions are studied numerically by using mean-field equations for the steady-state case. Under some restrictions on the rate constants and ratio of reactants pressures authors of [7] derived approximate analytical formulas to describe dynamics of $2A + B_2 \rightarrow 2AB$ reaction with spillover effect. In [15,16], the spillover effect in monomer-monomer, $A_1 + A_2 \rightarrow A_1A_2$, and dimer-dimer, $2A_2 + B_2 \rightarrow 2A_2B$, reactions are studied numerically by applying mean-field models based on the Fick and Gorban surface diffusion mechanisms [18], respectively. Using analytical methods and scaling concepts a model for steady-state uni-molecular reactions on the supported catalysts including reactant adsorption, desorption, and diffusion of adsorbed particles is examined in [2].

In this paper, we consider the bimolecular $A_1 + A_2 \rightarrow A_1A_2$ surface reaction proceeding on supported catalysts by using three models. The first of them is a revised monomer-monomer surface reactions model studied in [15]. It is described by PDEs and contrary to [15] is based on Gorban's surface diffusion mechanism [18]. A simplified model based on ODEs is derived by averaging of the revised PDEs model. The third mixed model contains PDEs for the bulk diffusion of both reactants and ODEs for the surface reaction and adsorbates diffusion.

Adsorption, desorption, and surface diffusion are allowed to proceed at a constant temperature and the product desorption is assumed to be instantaneous. We consider two adsorption cases of reactants A_1 and A_2: (i) both reactants adsorb only on the inactive support, (ii) one of reactants adsorbs on the catalyst particle while the other one adsorbs on the inactive in reaction support.

The goal of this paper is the comparison of the influence of the surface diffusivity, jump rate of adsorbed particles across the support-catalyst interface, and catalytic

particle size on the reactivity of supported catalysts determined by using three models mentioned above.

The paper is organized as follows. In Sect. 2 we present the model. In Sect. 3 we discuss numerical results. A summary of main results in Sect. 4 concludes the paper.

2 The models

We study the bimolecular reaction, $A_1 + A_2 \rightarrow A_1A_2$, proceeding on supported catalysts by using three mean-field models. The first of them is based on PDEs for concentrations of reacting species and product particles (refer to as PDEs model). To derive the second (ODEs) model we reduce the PDEs system to the ODEs by averaging of the PDEs model. Having derived two first models we construct the mixed one (refer to as Mixed model).

2.1 The PDEs model

In this section, we derive the PDEs model and consider the case where reactants A_1, A_2 and their reaction product $B = A_1A_2$ of concentrations $a_1(t, x)$, $a_2(t, x)$, and $b(t, x)$ occupy a bounded domain $\Omega = \{x = (x_1, x_2, x_3) : x_i \in [0, l],\ i = 1, 2, 3\}$ with boundary $\tilde{S} = S_1 \cup S_2$, where $S_2 = \{x = (x_1, x_2, x_3) : x_i \in [0, l],\ i = 1, 3,\ x_2 = 0\}$ and $S_1 = \tilde{S} \setminus S_2$. Here t is time, x is a position, S_2 is the surface of the adsorbent, and S_1 is a surface impermeable to the reactants and product. Obviously, $x_2 > 0$ for S_1.

Assume that $S_2 = S_{22} \cup S_{21}$ where $S_{22} = \{(x_1, x_2, x_3) : x_1 \in [0, x_*),\ x_2 = 0,\ x_3 \in [0, l]\}$ and $S_{21} = \{(x_1, x_2, x_3) : x_1 \in (x_*, l],\ x_2 = 0,\ x_3 \in [0, l]\}$, $x_* \in (0, l)$, are strips consisting of the active and inactive in reaction adsorption sites of densities $s_2(x)$, $x = (x_1, x_3) \in S_{22}$, and $s_1(x)$, $x = (x_1, x_3) \in S_{21}$, respectively (Fig. 1).

According to Langmuir–Hinshelwood the surface reaction $A_1 + A_2 \rightarrow A_1A_2$ occurs via steps

$$A_1 + S \underset{k_{-1i}}{\overset{k_{1i}}{\rightleftarrows}} A_1S,\ A_2 + S \underset{k_{-2i}}{\overset{k_{2i}}{\rightleftarrows}} A_2S,\ A_1S + A_2S \overset{k_{32}}{\rightarrow} A_1A_2 + 2S, \quad i = 1, 2.$$

Here S is the vacant adsorption site, k_{ji} and k_{-ji} are the adsorption and desorption rates constants ($i = 1$ for inactive site, $i = 2$ for active one) of reactants A_1 and A_2, k_{32} is the reaction between adsorbates A_1S and A_2S rate constant.

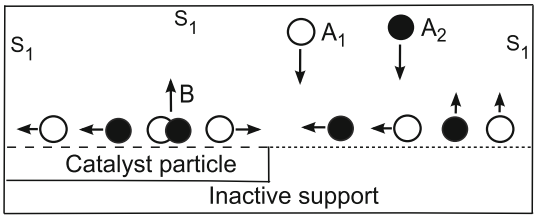

Fig. 1 Schematic representation of the model for the supported catalyst. *Dashed line* S_{22}, *dotted line* S_{21}, $S_2 = S_{22} \cup S_{21}$

Let $u_{i2} = s_2\theta_{i2}$ and $u_{i1} = s_1\theta_{i1}$ ($\theta_{i1},\ \theta_{i2} \in (0, 1)$) be concentrations of the active and inactive sites occupied by the adsorbed molecules of reactant A_i at moment t. It is evident that functions u_{i1} and u_{i2} present density of particles of species A_iS bound to sites of type i that are located at point x at moment t. Current advances in nanotechnology made it possible to produce nanopatterned surfaces with assumed geometric properties and to study their reactivity [9]. In Sect. 3, we specify $s_1(x)$ and $s_2(x)$ and for numerical study consider two distinct types of adsorption sites arrangement.

Let κ_{i1} and κ_{i2} be the surface diffusivity for particles of adsorbate A_iS located at the active and inactive part of catalyst surface, respectively. To simplify the model we restrict ourselves to the case where densities s_1 and s_2 do not depend variable x_3 and the initial values a_1^0, a_2^0, and b^0 of concentrations a_1, a_2, and b are constants. In this case we can reduce the three-dimensional problem into two-dimensional one. Let $\lambda_{1,12}$ and $\lambda_{1,22}$ be constants of the jump rates via the catalyst-support interface x_* of escaped particles of species A_1S and A_2S from the active position $x_* - 0$ into the nearest-neighbour vacant inactive site $x_* + 0$. Similarly, $\lambda_{2,11}$ and $\lambda_{2,21}$ are constants of the jump rates via the catalyst-support interface of escaped particles of species A_1S and A_2S from the inactive position $x_* + 0$ into the nearest-neighbour vacant active site $x_* - 0$. Assuming that product desorption is instantaneous and using mass action law and the surface diffusion mechanism based on the particle jumping into a nearest vacant adsorption site [18],

$$q_{ji} = -\kappa_{ji}\big\{(s_i - u_{1i} - u_{2i} - u_{3i})\nabla u_{ji} - u_{ji}\nabla(s_i - u_{1i} - u_{2i} - u_{3i})\big\},$$

we derive the following system for densities $u_{ij}(t, x_1)$, $i,\ j = 1, 2$,

$$\begin{aligned}
&\partial_t u_{i1} = k_{i1}a_i(s_1 - u_{11} - u_{21}) - k_{-i1}u_{i1}\\
&\qquad + \kappa_{i1}\big((s_1 - u_{3-i1})\partial^2_{x_1x_1}u_{i1} - u_{i1}\partial^2_{x_1x_1}(s_1 - u_{3-i1})\big),\\
&\quad x_1 \in (x_*, l),\ t > 0,\\
&\partial_t u_{i2} = k_{i2}a_i(s_2 - u_{12} - u_{22}) - k_{-i2}u_{i2} - k_{32}u_{12}u_{22}\\
&\qquad + \kappa_{i2}\big((s_2 - u_{3-i2})\partial^2_{x_1x_1}u_{i2} - u_{i2}\partial^2_{x_1x_1}(s_2 - u_{3-i2})\big),\\
&\quad x_1 \in (0, x_*),\ t > 0.
\end{aligned} \tag{1}$$

Here $i = 1, 2$ and ∇ is the gradient operator. We add to this system the initial

$$u_{ij}(0, x_1) = 0, \quad i, j = 1, 2, \tag{2}$$

and boundary conditions at points $x_1 = 0,\ x_1 = x_*$, and $x_1 = l$,

$$\begin{aligned}
&\partial_{x_1}u_{12}|_{x_1=0} = \partial_{x_1}u_{22}|_{x_1=0} = 0,\\
&\partial_{x_1}u_{11}|_{x_1=l} = \partial_{x_1}u_{21}|_{x_1=l} = 0,\\
&\kappa_{11}\big((s_1 - u_{21})\partial_{x_1}u_{11} - u_{11}\partial_{x_1}(s_1 - u_{21})\big)\\
&\quad = \kappa_{12}\big((s_2 - u_{22})\partial_{x_1}u_{12} - u_{12}\partial_{x_1}(s_2 - u_{22})\big)\\
&\quad = \lambda_{2,11}\kappa_{11}u_{11}(s_2 - u_{12} - u_{22}) - \lambda_{1,12}\kappa_{12}u_{12}(s_1 - u_{11} - u_{21}),
\end{aligned} \tag{3}$$

$$\begin{aligned}
&\kappa_{21}\big((s_1-u_{11})\partial_{x_1}u_{21}-u_{21}\partial_{x_1}(s_1-u_{11})\big)\\
&\quad=\kappa_{22}\big((s_2-u_{12})\partial_{x_1}u_{22}-u_{22}\partial_{x_1}(s_2-u_{12})\big)\\
&\quad=\lambda_{2,21}\kappa_{21}u_{21}(s_2-u_{12}-u_{22})-\lambda_{1,22}\kappa_{22}u_{22}(s_1-u_{11}-u_{21}).
\end{aligned}\tag{4}$$

We also join diffusion equations for concentrations of both reactants A_1, A_2 and product B,

$$\begin{aligned}
&\partial_t a_1=\kappa_{a_1}\Big(\frac{\partial^2 a_1}{\partial x_1^2}+\frac{\partial^2 a_1}{\partial x_2^2}\Big),\ (x_1,x_2)\in(0,l)\times(0,l),\ t>0,\\
&\partial_n a_1|_{S_1}=0,\quad t>0,\\
&\kappa_{a_1}\partial_n a_1=-\big(k_{11}a_1(s_1-u_{11}-u_{21})-k_{-11}u_{11}\big),\\
&\quad x_2=0,\ x_1\in(x_*,l),\quad t>0,\\
&\kappa_{a_1}\partial_n a_1=-\big(k_{12}a_1(s_2-u_{12}-u_{22})-k_{-12}u_{12}\big),\\
&\quad x_2=0,\ x_1\in(0,x_*),\quad t>0,\\
&a_1|_{t=0}=a_1^0,\quad (x_1,x_2)\in(0,l)\times(0,l),
\end{aligned}\tag{5}$$

$$\begin{aligned}
&\partial_t a_2=\kappa_{a_2}\Big(\frac{\partial^2 a_2}{\partial x_1^2}+\frac{\partial^2 a_2}{\partial x_2^2}\Big),\quad (x_1,x_2)\in(0,l)\times(0,l),\ t>0,\\
&\partial_n a_2|_{S_1}=0,\quad t>0,\\
&\kappa_{a_2}\partial_n a_2=-\big(k_{21}a_2(s_1-u_{11}-u_{21})-k_{-21}u_{21}\big),\\
&\quad x_2=0,\ x_1\in(x_*,l),\quad t>0,\\
&\kappa_{a_2}\partial_n a_2=-\big(k_{22}a_2(s_2-u_{12}-u_{22})-k_{-22}u_{22}\big),\\
&\quad x_2=0,\ x_1\in(0,x_*),\quad t>0,\\
&a_2|_{t=0}=a_2^0,\quad (x_1,x_2)\in(0,l)\times(0,l),
\end{aligned}\tag{6}$$

$$\begin{aligned}
&\partial_t b=\kappa_b\Big(\frac{\partial^2 b}{\partial x_1^2}+\frac{\partial^2 b}{\partial x_2^2}\Big),\quad (x_1,x_2)\in(0,l)\times(0,l),\\
&\partial_n b|_{S_1}=0,\quad t>0,\\
&\kappa_b\partial_n b=0,\quad x_2=0,\ x_1\in(x_*,l),\quad t>0,\\
&\kappa_b\partial_n b=k_{32}u_{12}u_{22},\quad x_2=0,\ x_1\in(0,x_*),\quad t>0,\\
&b|_{t=0}=0,\quad (x_1,x_2)\in(0,l)\times(0,l).
\end{aligned}\tag{7}$$

Here $\partial_n a_1$, $\partial_n a_2$, and $\partial_n b$ are the outward normal derivatives whereas s_2 and s_1 in Eqs. (1), (4)–(6) are densities of the active and inactive in reaction adsorption sites. Eqs. (1)–(7) compose the PDEs model.

2.2 The ODEs model

In this section, by using the averaging procedure over intervals (x_*, l) and $(0, x_*)$ for the first and second equation of system (1) and over domain $\Omega := [0, l]\times[0, l]$ for Eqs.

(5)–(7), we derive a simplified model in the case where concentrations of adsorption sites s_1 and s_2 are constants. To simplified Eqs. (1)–(7) we first determine the average values of a_i, u_{i2}, and u_{i1} as $\int_0^l \int_0^l a_i \, dx_1 \, dx_2/l^2$, $\int_o^{x_*} u_{i2} \, dx_1/x_*$, $\int_{x_*}^l u_{i1} \, dx_1/(l-x_*)$, $i = 1, 2$, respectively, and note that the diffusion term in both Eqs. (1) can be written in the divergence form of the diffusion flux q_{ij} while the corresponding term in Eqs. (5) and (6) already possesses the divergence form. Then we integrate Eqs. (1), (5)–(7), apply the Gauss–Ostrogradsky divergence theorem to the diffusion terms, use the corresponding boundary conditions with all functions on their right-hand sides replaced by the corresponding average values, and employ the same notations for averaged functions to get the system of ODEs:

$$\begin{aligned} a_i' &= -(l-x_*)\big(k_{i1}a_i(s_1-u_{11}-u_{21})-k_{-i1}u_{i1}\big)/l^2 \\ &\quad -x_*\big(k_{i2}a_i(s_2-u_{12}-u_{22})-k_{-12}u_{i2}\big)/l^2, \quad a_i(0)=a_i^0, \quad i=1,2, \end{aligned} \tag{8}$$

$$\begin{aligned} u_{i1}' &= k_{i1}a_i(s_1-u_{11}-u_{21})-k_{-i1}u_{i1} \\ &\quad +(l-x_*)^{-1}\big(\lambda_{1,i2}\kappa_{i2}u_{i2}(s_1-u_{11}-u_{21})-\lambda_{2,i1}\kappa_{i1}u_{i1}(s_2-u_{12}-u_{22})\big), \\ &\quad u_{i1}(0)=0, \quad i=1,2; \\ u_{i2}' &= k_{i2}a_i(s_2-u_{12}-u_{22})-k_{-i2}u_{i2}-k_{32}u_{12}u_{22} \\ &\quad +(x_*)^{-1}\big(\lambda_{2,i1}u_{i1}\kappa_{i1}(s_2-u_{12}-u_{22})-\lambda_{1,i2}\kappa_{i2}u_{i2}(s_1-u_{11}-u_{21})\big) \\ &\quad u_{i2}(0)=0, \quad i=1,2, \end{aligned} \tag{9}$$

$$b' = x_* k_{32} u_{12} u_{22}, \quad b(0) = 0. \tag{10}$$

Equations (8)–(10) compose the ODEs model.

2.3 The mixed model

In this section, having derived equations for the first two models, we construct the Mixed model for the case of constant s_1 and s_2. To do this we consider Eqs. (5)–(7) for bulk concentrations a_1, a_2, and b with u_{i1} and u_{i2} in the boundary conditions replaced by their averaged values $\int_{x_*}^l u_{i1} \, dx_1/(l-x_*)$ and $\int_0^{x_*} u_{i2} \, dx_1/x_*$ and Eqs. (9) for averaged values of u_{i1} and u_{i2} with a_i replaced by $\int_{x_*}^l a_i \, dx_1/(l-x_*)$ and $\int_0^{x_*} a_i \, dx_1/x_*$, respectively. These revised Eqs. (5)–(7) and (9) compose the Mixed model.

The PDEs, ODEs, and Mixed models possess two mass conservation laws:

$$\int_\Omega (a_i + b)\, dx + \int_0^{x_*} u_{i2} \, dx_1 + \int_{x_*}^{l} u_{i1} \, dx_1 = \int_\Omega (a_i^0 + b^0)\, dx, \quad i = 1, 2.$$

The main characteristic we study is the surface reactivity (turnover frequency or rate) determined by the equation

$$z = \frac{\int_0^{x_*} k_{32} u_{12} u_{22}\, \mathrm{d}x_1}{x_* s_2}. \tag{11}$$

Using the dimensionless variables

$$\begin{aligned}
&\bar{t} = t/T, \quad \bar{x}_i = x_i/l, \quad \bar{a}_i = a_i/a_*, \quad \bar{b} = b/a_*, \quad \bar{s}_i = s_i/(la_*),\\
&\bar{u}_{ij} = u_{ij}/(la_*), \bar{k}_{ij} = k_{ij} T a_*, \quad \bar{k}_{-ij} = k_{-ij} T, \quad \bar{k}_{3j} = k_{3j} T,\\
&\bar{\kappa}_{a_i} = \kappa_{a_i} T/l^2, \quad \bar{\kappa}_b = \kappa_b T/l^2, \quad \bar{\kappa}_{ij} = \kappa_{ij} T a_*/l,\\
&\bar{\lambda}_{1,j2} = l\lambda_{1,j2}, \quad \bar{\lambda}_{2,j1} = l\lambda_{2,j1},
\end{aligned} \tag{12}$$

where $i, j = 1, 2$ and T, l, a_* are the characteristic dimensional units, we rewrite Eqs. (1)–(10) in the same form, but now in the non-dimensional form expressed by using the dimensionless (overscored) quantities. Therefore, for simplicity in what follows, we omit the bar and treat system (1)–(10) as the non-dimensional with dimensionless $l = 1$. Numerical values of scales T, l, and a_* are given in Sect. 3.

In what follows we study Eqs. (1)–(4) and (9) with given constant values of a_1, a_2 and full systems (1)–(7) (PDEs model), (8)–(10) (ODEs model), and equations of the Mixed model in the following two adsorption cases of the reactants A_1 and A_2:

(i) both reactants adsorb only on the inactive in reaction interval $(x_*, 1]$,
(ii) reactant A_1 adsorbs on the interval $[x_*, 1]$, while the A_2 adsorbs on the $(0, x_*]$.

Hence, in case (i) we have $k_{12} = k_{22} = 0$, while in case (ii) $k_{12} = k_{21} = 0$.

3 Numerical results

System (1)–(4) with given values of a_1 and a_2 at the surface S_2 was solved numerically using an implicit difference scheme. To solve system (1)–(7) numerically we used an implicit difference scheme based on the alternating direction method [19]. Systems of ODEs were solved by standard MATLAB ODE solvers, viz. ode45 and ode113, ode15s [20,21].

For all calculations we used the following dimensional data:

$$\begin{aligned}
&T = 1\ \mathrm{s}, \quad l = 10^{-1}\ \mathrm{cm}, \quad a_* = 10^{-11}\ \mathrm{mol\,cm^{-3}},\\
&s_* = la_* = 10^{-12}\ \mathrm{mol\,cm^{-2}}, \quad k_{ij} \in [10^9, 10^{11}]\ \mathrm{cm^3\,mol^{-1}\,s^{-1}},\\
&k_{-ij},\ k \in [3 \times 10^{-3}, 1]\ \mathrm{s^{-1}}, \quad \kappa_{a_i}, \kappa_b \in [5 \times 10^{-7}, 10^{-3}]\ \mathrm{cm^2\,s^{-1}}.
\end{aligned} \tag{13}$$

Dimensional numerical values of the other parameters directly follow from Eqs. (12) and (13). In the case where values of k_{ij}, κ_{ij}, and $\lambda_{i,jn}$ for all values of indices are equal, we use $k = k_{ij}$, $\kappa = \kappa_{ij}$, and $\lambda = \lambda_{i,jn}$ for short.

The following values of dimensionless parameters (overbar on the quantities is omitted) excluding those given in captions were used in calculations:

$$
\begin{aligned}
&k_{ji} = 1.66 \times 10^{-2}, \quad k_{-ji} = 1.66 \times 10^{-3}, \quad k_{32} = 0.1,\\
&\kappa_{ji} = 0.1, \quad \lambda_{n,ji} = 1, \quad n, i, j = 1, 2,\\
&\kappa_{a_1} = \kappa_{a_2} = \kappa_b = 0.1, \quad x_* = 0.2.
\end{aligned} \tag{14}
$$

The model values of dimensionless k_{ij}, κ_{ij}, and $\lambda_{i,jn}$ are given in the captions of figures.

To study the influence of the adsorption sites arrangement we use for calculations two different distributions of the adsorption sites (i) $s_1 = s_2 = 1$ and (ii) $s_2 = s_1(1/x_* - 1)$, $s_1 = 1$. In the first case, the total amounts of the active and inactive sites for $x_* \neq 0.5$ are different. In the second case these amounts are equal, i.e., $\int_0^{x_*} s_2 \, dx_1 = \int_{x_*}^1 s_1 \, dx_1$. Contrary to the first arrangement, density of active sites distribution, s_2, depends on the catalyst particle size x_* in the case (ii). It grows or decreases as x_* decreases or increases, respectively. But for $x_* = 0.5$, $s_2 = s_1 = 1$ in both arrangements of the adsorption sites. Using the second arrangement we study the influence of the catalytic particle size-dependent distribution of the active sites on the surface reactivity provided that the total amount of the active and inactive adsorption sites is the same.

We begin with discussion of numerical results for systems (1)–(4) and (9) with given constant values of a_1 and a_2. Numerical results are illustrated in Figs. 2, 3, 4 in the case where concentrations of active and inactive sites are equal, i.e. $s_1 = s_2$. Figs. 5, 6 correspond to the case of equal total amount of active and inactive sites. Comparison of the turn-over rate determined by the full PDEs, ODEs, and Mixed models is given in the last Fig. 7.

In Fig. 2 the comparison of turn-over rate $z(t)$ determined by systems (1)–(4) and (9) for different values of jump rate constant $\lambda_{2,11} = \lambda_{2,21}$ of escaped adsorbate particles

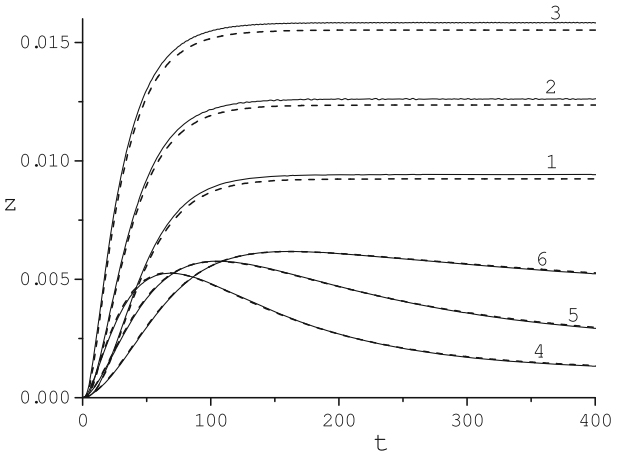

Fig. 2 Effect of variation of jump rate constant λ on the turnover rate $z(t)$ determined by the PDEs model (*dashed line*) and by ODEs model (*solid line*) with $a_1 = a_2 = 1$ for densities $s_1 = s_2 = 1$ in the cases $k_{12} = k_{22} = 0$, $k_{11} = k_{21} = 0.0166$ (*curves* **1**, **2**, **3**) and $k_{12} = k_{21} = 0$, $k_{11} = k_{22} = 0.0166$ (*curves* **4**, **5**, **6**). Values of $\lambda_{2,11} = \lambda_{2,21}$ are: 0.5 **(1)** and **(4)**, 1 **(2)** and **(5)**, 2 **(3)** and **(6)**

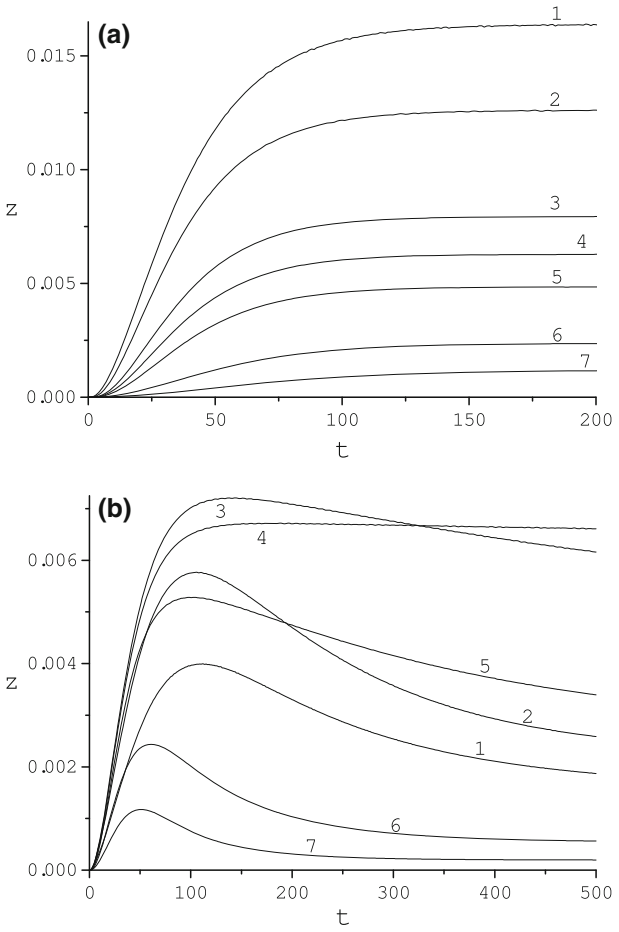

Fig. 3 Dependence of turnover rate $z(t)$ determined by the ODEs model with $a_1 = a_2 = 1$ and densities $s_1 = s_2 = 1$ on the active interval length x_*: 0.1 **(1)**, 0.2 **(2)**, 0.4 **(3)**, 0.5 **(4)**, 0.6 **(5)**, 0.8 **(6)**, 0.9 **(7)**. **(a)** $k_{12} = k_{22} = 0, k_{11} = k_{21} = 0.0166$, **(b)** $k_{12} = k_{21} = 0, k_{11} = k_{22} = 0.0166$

across the catalyst-support interface is given. Curves 1, 2, 3 and 4, 5, 6 correspond to different arrangement of adsorption sites. Curves 1, 2, 3 are plotted for the cases where both reactants adsorb on the support $(x_*, 1)$ with $x_* = 0.2$ while curves 4, 5, 6 are drawn in the case where A_1 and A_2 adsorb on the support and the active interval, respectively. This figure shows that the averaged model (9) provides a good approximation of surface reactivity $z(t)$ (maximal different between curves determined by PDEs and ODEs models is less than 3% for curves 1, 2, 3 and is negligible for the other three ones).

Figure 3 illustrates the influence of the active interval size x_* on the behaviour of the turn-over rate $z(t)$ for $k_{12} = k_{22} = 0, k_{11} = k_{21} = 0.0166$ (Fig. 3a) and $k_{12} = k_{21} = 0, k_{11} = k_{22} = 0.0166$ (Fig. 3b). In case where both reactants adsorb on the support, function $z(t)$ is monotonic in time and grows as size x_* increases.

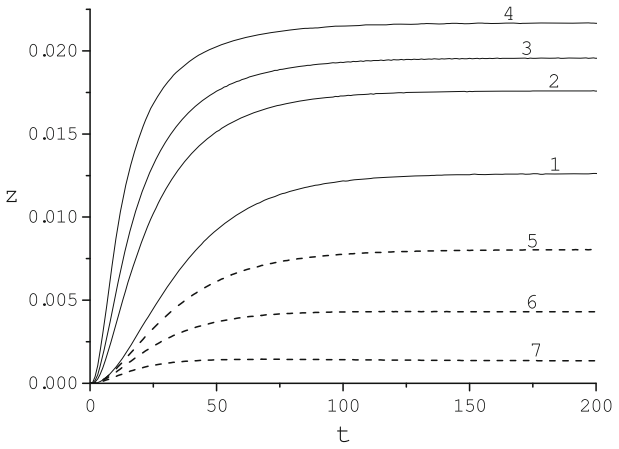

Fig. 4 Effect of the surface diffusivity on the turnover rate $z(t)$ determined by the ODEs model with $a_1 = a_2 = 1$ for densities $s_2 = s_1 = 1$ in case $k_{12} = k_{22} = 0$, $k_{11} = k_{21} = 0.0166$. *Solid line* $\kappa_{12} = \kappa_{22} = 0.1$, $\kappa_{11} = \kappa_{21}$: 0.1 **(1)**, 0.3 **(2)**, 0.5 **(3)**, 1 **(4)**; *dashed line* $\kappa_{11} = \kappa_{22} = 0.1$, $\kappa_{12} = \kappa_{21}$: 0.3 **(5)**, 0.5 **(6)**, 1 **(7)**

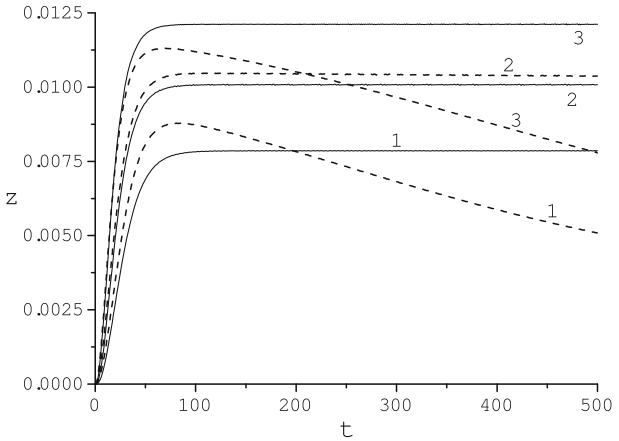

Fig. 5 Influence of the parameter $\lambda_{2,11} = \lambda_{2,21}$: 0.5 **(1)**, 1 **(2)**, 2 **(3)** on the turnover rate $z(t)$ determined by the ODEs model with densities $a_1 = a_2 = 1$ and $s_2 = s_1(1/x_* - 1)$, $s_1 = 1$ in cases $k_{12} = k_{22} = 0$, $k_{11} = k_{21} = 0.0166$ (*solid line*) and $k_{12} = k_{21} = 0$, $k_{11} = k_{22} = 0.0166$ (*dashed line*)

In case of reactants adsorption on different intervals, function $z(t)$ grows in time, possesses maximum, and then decreases to a steady-state value depending on the other parameters. Figure 3b also shows that z as function of parameter x_* also possesses a maximum in the case of reactants adsorption on different intervals.

Effect of varying surface diffusivity κ_{ij} on function $z(t)$ is depicted in Fig. 4. Curves 1, 2, 3, and 4 correspond to different values of $\kappa_{11} = \kappa_{21}$ ($\kappa_{12} = \kappa_{22} = 0.1$) and curves 5, 6, and 7 are drown for varying $\kappa_{12} = \kappa_{21}$($\kappa_{11} = \kappa_{22} = 0.1$). Plots in this figure demonstrate the increase of $z(t)$ as $\kappa_{11} = \kappa_{21}$ grows and its decrease as $\kappa_{12} = \kappa_{21}$ increases. Moreover, function $z(t)$ is monotonic in time. Our calculations also show a

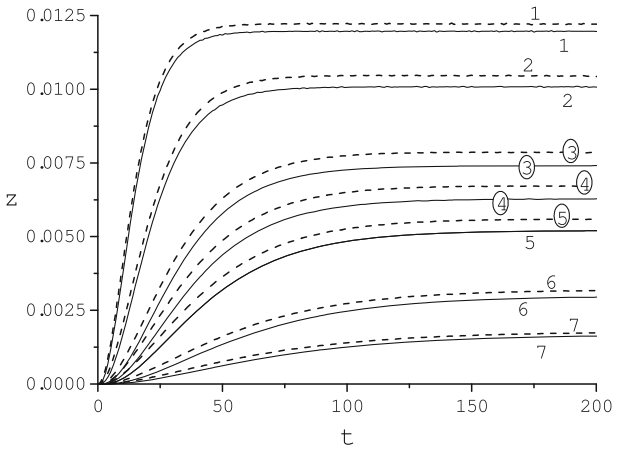

Fig. 6 Effect of variation of the active interval length x_* on the turnover rate $z(t)$ determined by the ODEs model with densities $a_1 = a_2 = 1$ and $s_2 = s_1(1/x_* - 1)$, $s_1 = 1$ in cases $k_{12} = k_{22} = 0$, $k_{11} = k_{21} = 0.0166$ (*solid line*) and $k_{12} = k_{21} = 0$, $k_{11} = k_{22} = 0.0166$ (*dashed line*). Values of x_*: 0.1 **(1)**, 0.2 **(2)**, 0.4 **(3)**, 0.5 **(4)**, 0.6 **(5)**, 0.8 **(6)**, 0.9 **(7)**

similar behaviour of $z(t)$ determined for the case of reactants adsorption on different intervals.

Comparison of different influence of varying parameter $\lambda_{2,11} = \lambda_{2,21}$ on the turnover rate $z(t)$ in case of two different types of reactants adsorption is depicted in Fig. 5. For small values of $\lambda_{2,11} = \lambda_{2,21}$ and small time, function $z(t)$ corresponding to the case of reactants adsorption on different intervals is larger than that determined for the case where both reactants adsorb on the support. For large time this behaviour is opposite. For large values of $\lambda_{2,11} = \lambda_{2,21}$ function $z(t)$ corresponding to the case of reactants adsorption on different intervals is smaller than that determined for reactants adsorption on the support. In the case of reactants adsorption on different intervals, function $z(t)$ possesses maximum in time, while in the other case it is a monotonic function of time.

Figure 6 depicts the dependence of the turn-over rate on the active interval size, x_*. Solid lines correspond to the adsorption of both reactants on the support while dashed lines illustrate function $z(t)$ determined for reactants adsorption on different intervals. In both cases function $z(t)$ is monotone in time and increases as parameter $k_{11} = k_{21}$ (see solid lines) or $k_{11} = k_{22}$ (dashed lines) grows. Moreover, function $z(t)$ corresponding to the case of reactants adsorption on different intervals is larger than that determined for both reactants adsorption on the support. Maximal difference between values of $z(t)$ corresponding to two types of reactants adsorption is about 7% from values of $z(t)$ determined for adsorption of both reactants on the support.

The different influence of the bulk diffusivity of reactants on the turn-over rate determined by PDEs, ODEs, and Mixed models is depicted in Fig. 7 for $s_1 = s_2 = 1$ and adsorption of both reactants on the support (Fig. 7a) and for the reactants adsorption on different intervals (Fig. 7b). This figure shows that the ODEs model well approximates the turn-over rate, $z(t)$, only if the bulk diffusivity of both reactants is large. In case of small reactants bulk diffusivity, function $z(t)$ corresponding to

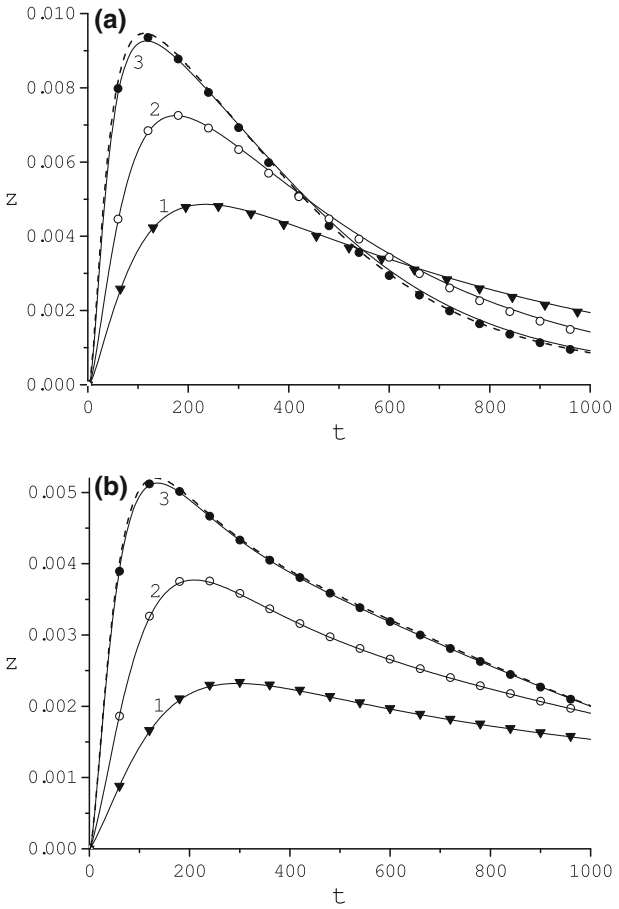

Fig. 7 Comparison of function $z(t)$ determined by the ODEs (*dashed line*), PDEs (*solid line*), and mixed (*symbol*) models at three values of the reactants diffusivity $\kappa_{a_1} = \kappa_{a_2}$: 0.001 **(1)** and *filled inverted triangle*, 0.003 **(2)** and *open circle*, 0.1 **(3)** and *filled circle* in cases $k_{12} = k_{22} = 0$, $k_{11} = k_{21} = 0.0166$ (Fig. 6a) and $k_{12} = k_{21} = 0$, $k_{11} = k_{22} = 0.0166$ (Fig. 6b) with $a_1^0(x_1, x_2) = a_2^0(x_1, x_2) = 1$ and densities $s_1 = s_2 = 1$

the ODEs model dramatically differs from that determined by the PDEs model. The mixed model provides a very good approximation of $z(t)$ for all considered values of the bulk reactants diffusivity.

4 Conclusions

To conclude the paper, we summarise the main results. In this paper, using three (PDEs, ODEs, and Mixed) phenomenological models we studied numerically bimolecular surface reactions proceeding on the supported catalysts. It is assumed that the support is inactive in reaction. The PDEs model includes the bulk diffusion of both reactants from a bounded impermeable vessel towards the adsorbent and the product bulk one into the same vessel, adsorption and desorption of molecules of both reactants and

rapid product desorption, surface diffusion of adsorbed particles described by the diffusion flux based on the particle jumping into a nearest vacant adsorption site [18]. The ODEs model is derived by averaging of the PDEs. Two different arrangements of adsorption sites were used: (i) concentrations of adsorption sites of the support and catalyst particle are equal, (ii) the total amount of adsorption sites of the support and catalyst particle are the same. Two cases of reactants adsorption are considered: (i) both reactants adsorb on the support only, (ii) one reactant adsorbs on the support while the other one adsorbs on the active in reaction catalyst particle.

Inactive in reaction sites, due to possibility of adsorption of at least one of reactants, diffusion of adsorbed particles, and their jump across the catalyst-support interface constitute an additional (to the adsorption) spillover channel transporting particles onto active sites.

The main characteristic we studied was the catalyst particle specific conversion rate (turn-over rate) of molecules of both reactants into the product ones. We compared PDEs, ODEs, and Mixed models and demonstrate that:

1. ODEs model (9) with given concentrations of both reactants is good enough for evaluation of the reactivity of composite catalysts.
2. ODEs (8)–(9) provide a good model for evaluation of the surface reactivity of the composite catalysts only if the reactants bulk diffusivity is large.
3. The mixed model practically very well describes the turn-over rate $z(t)$ of supported catalysts for all values of kinetic parameters.
   We analysed the spillover effects determined by system (9) with given concentration of both reactants, a_1 and a_2, on the turn-over rate, $z(t)$, under different conditions and found that:
4. The size of the active interval, x_*, and adsorption type of both reactants strongly influence the turn-over rate:
   4.1. If both reactants adsorb only on the support then in both cases of active sites arrangement ($s_1 = s_2$ and $s_2 = s_1(1/x_* - 1)$) function z determined by system (9) grows as size, x_*, decreases and is monotone in time.
   4.2. In case of reactants adsorption on different intervals and $s_1 = s_2$, function $z(t)$ grows as x_* decreases. But it is non-monotonic in time (possesses maximum value and then tends to a positive asymptotic value depending on the other parameters) if $s_2 = s_1(1/x_* - 1)$.
5. For both arrangements of adsorption active sites ($s_1 = s_2$ and $s_2 - s_1(1/x_* - 1)$) and fixed $\kappa_{12} = \kappa_{22}$, the increase of diffusion coefficient $\kappa_{11} = \kappa_{21}$ increases $z(t)$. But for fixed $\kappa_{11} = \kappa_{22}$ the increase of the surface diffusivity $\kappa_{12} = \kappa_{21}$ decreases $z(t)$.
6. If both reactants adsorb only on the support and $\lambda_{1,12} = \lambda_{1,22}$ is fixed, then for both adsorption sites arrangements function $z(t)$ is monotone in time and grows as jump rate constant $\lambda_{2,11} = \lambda_{2,21}$ increases. But if reactants adsorb on different intervals, then for both arrangements of adsorption sites behaviour of function $z(t)$ is convoluted in time (not monotone).

Results of simulations let us to think that the Mixed model presented here is able to describe qualitatively processes that proceed at constant temperature during monomer-monomer reactions on supported catalysts.

References

1. D.Y. Murzin, Ind. Eng. Chem. Res. **44**, 1688 (2005)
2. T.G. Mattos, F.D.A. Aarão Reis, J. Catal. **263**, 67 (2009)
3. L.J. Broadbelt, R.Q. Snurr, Appl. Catal. A **200**, 23 (2000)
4. V.P. Zhdanov, B. Kasemo, Surf. Sci. Rep. **39**, 25 (2000)
5. H. Lynggaard, A. Andreasen, C. Stegelmann, P. Stoltze, Prog. Surf. Sci. **77**, 71 (2004)
6. L. Cwiklik, B. Jagoda-Cwiklik, M. Frankowicz. arXiv:physics/0409153v2 [physics.chem-ph] 20 Jan 2005
7. T.G. Mattos, F.D.A. Aarão Reis. arXiv:0906.3063v1 [cond-mat.stat-mech] 17 Jun 2009
8. L. Cwiklik, B. Jagoda-Cwiklik, M. Frankowicz, Appl. Surf. Sci. **252**, 778 (2005)
9. L. Cwiklik, B. Jagoda-Cwiklik, M. Frankowicz, Surf. Sci. **572**, 318 (2004)
10. E.V. Kovaliov, E.D. Resnyanskii, V.I. Elokhin, B.S. Bal'zhinimaev, A.V. Myshlyatsev, Phys. Chem. Chem. Phys. **5**, 784 (2003)
11. L. Cwiklik. arXiv:0710.4785v1 [cond-mat.mtrl-sci] 25 Oct 2007
12. L. Cwiklik, Chem. Phys. Lett. **449**, 304 (2007)
13. V. Skakauskas, P. Katauskis, J. Math. Chem. **51**, 492 (2013)
14. V. Skakauskas, P. Katauskis, J. Math. Chem. **51**, 1654 (2013)
15. V. Skakauskas, P. Katauskis, J. Math. Chem. **52**, 1350 (2014)
16. V. Skakauskas, P. Katauskis, J. Math. Chem. (2014). doi:10.1007/s10910-014-0440-2
17. V.P. Zhdanov, B. Kasemo, J. Catal. **170**, 377 (1997)
18. A.N. Gorban, H.P. Sargsyan, H.A. Wahab, Math. Model. Nat. Phenom. **6**, 184262 (2011). arXiv:1012.2908v4 [cond-mat.mtrl-sci]
19. A.A. Samarskii, *The theory of difference schemes* (Marcel Dekker, New York, 2001)
20. W.H. Press, S.A. Teukolsky, W.T. Vetterling, B.P. Flannery, *Numerical recipes: the art of scientific computing*, 3rd edn. (Cambridge University Press, Cambridge, 2007)
21. L.F. Shampine, I. Gladwell, S. Thompson, C. Beardah, *Solving ODEs with MATLAB* (Cambridge University Press, Cambridge, 2003)